Comparison between cold and hot network in a solar district cooling system

Journal of Physics: Conference Series **2893** (2024) 012031 doi:10.1088/1742-6596/2893/1/012031

Comparison between cold and hot network in a solar district cooling system

E. Ghirardi[1*], G. Brumana[1], G. Franchini[1]

[1] Department of Engineering and Applied Science, University of Bergamo, Dalmine, Italy

[*]E-mail: elisa.ghirardi@unibg.it

Abstract. Heat-powered absorption cooling have attracted attention in recent decades, especially in regions with hot and arid climates a higher availability of solar radiation, can be exploited in solar-assisted District Cooling (SDC) system to reduce costs. The paper proposes a comparison of two Solar District Cooling configurations powered by a PTC field with thermal storage and an absorption chiller. The first configuration, called cold network, has a large hot water storage tank slaved to a single chiller that produces all the chilled water that is distributed to the network; in the second configuration, called hot network, the water heated in the solar array is sent through the network directly to thermal storage tanks, located near the buildings to be served, where each agglomeration has its own chillers. A techno-economic optimization was performed for the two configurations by varying the Solar Fraction (SF), from 25% to 100%. When solar radiation is not sufficient to meet demand, an auxiliary electric chiller will be used. The results show that component size increases linearly with SF up to 75%. To achieve a fully renewable solution, components need to be significantly oversized. Generally, a SDC system in a centralized configuration offers improved performance and reduced distribution losses. However, this is not the case for a scenario with unitary SF, where the distribution network takes on an additional thermal reserve role.

1. Introduction

Building energy demand accounts for 36% of global electricity demand, with electric fans and air conditioners responsible for 20% of electricity consumption. Despite advancements in cooling technologies, CO_2 emissions have more than doubled in the last 30 years (1). One possibility to reduce energy consumption by up to 80 percent compared to conventional systems is the District Cooling System (DCS), a centralized system supplying thermal energy in the form of chilled water to be used for air conditioning, also increasing the economic feasibility of integration with renewable energy (2).

Recent studies have shown that the newest district systems (5th generation) may not be cost-effective when the load is mainly unbalanced on thermal or cooling demand (3). However, it has been reported that heat-powered absorption cooling can reduce the energy consumption of district heating systems by up to 70%, based on system design and modelling approaches (4). These systems have attracted attention in recent decades, especially in regions with hot and arid climates such as the Middle East and North Africa (MENA), as demonstrated by the largest DC market in 2019 (5). In addition, thanks to the higher availability of solar radiation, solar-assisted

District Cooling (SDC) may help increase performance and reduce costs. The most efficient configuration is based on 2sABS two-stage absorption chillers, whose COP is usually around 1.3-1.4, but a flow temperature above 150°C is required and thus a medium-concentration solar collector such as a PTC (6).

In recent years, studies have shown that there are many aspects to consider when designing district cooling systems in order to increase competitiveness and reduce costs (7). Most common configurations use centralised chilled water production (8) and the implementation of a chilled water tank can reduce costs by 40% according to Michaelides et al. and Al-Nini et al. (9,10). The importance of optimising individual components to maximise the potential of the network has been demonstrated by many authors, including Thakar et al.(11). The study presented by Shi et al. (12) analyses the impact of network design on efficiency in high-density cities such as Singapore, showing a cost difference of up to 90% in the worst case. One way to reduce the impact of the cooling system is to integrate it with other systems, such as district heating or combined heat and power. Dai et al. have shown that integration of DC into an electrical system can reduce wind reduction by 87% (13), and Lepiksaar et al. have also shown a reduction in primary energy demand for cooling (14).

As reported by Neri et al. (15), one of the most penalizing issues is the relatively small difference between the supply and return temperatures. It is worth mentioning the approaches that vary the distribution temperature, for example Zhang et al. in (16) proposed a variable temperature strategy to adapt to the outdoor temperature variation, reducing the energy consumption by almost 20%, or the strategy reported by Jangsten et al. that increases the supply temperature to increase the share of free cooling (17). However, only a few authors have studied distributed cooling production along the network. The work of Guelpa et al. (18) is cited, who studied the optimal location of distributed heat pumps, reducing the costs by about 7% compared to a centralized production. Similarly, Cozzini et al. considered a decentralized system of heat pumps in a district heating and cooling system (19).

To the best of the authors' knowledge, decentralized cold production using solar thermal energy has never been considered in district cooling design. Based on previous studies on solar cooling plants (20,21), it is proposed to compare a solar district cooling system with a cold or hot distribution network. The paper first presents the Trnsys models developed to reproduce the cooling load of a residential complex, the cooling plant and the district network. A techno-economic optimization was carried out with the GenOpt tool for the two configurations, varying the solar fraction (SF) up to a fully solar scenario.

2. Modelling and Optimization

The paper proposes a comparison of two Solar District Cooling configurations powered by a PTC field with thermal storages and absorption chillers, as resumed in Fig. 1. The first configuration, called cold network, has a large hot water storage tank slaved to a single chiller that produces all the chilled water that is distributed to the network; in the second configuration, called hot network, the water heated in the solar array is sent through the network directly to thermal storage tanks, located near the buildings to be served, where each agglomeration has its own chillers.

The solar collector efficiency is evaluated based on a quadratic efficiency equation (1) where CR is the concentration ratio equal to 60. The coefficients A, B and C (0.7719, 0.1803, and 0.0258 respectively) are the optical efficiency and the heat loss coefficient of first and second order. The fluid flow rate is set to maintain an outlet temperature as close to 180°C as possible. If

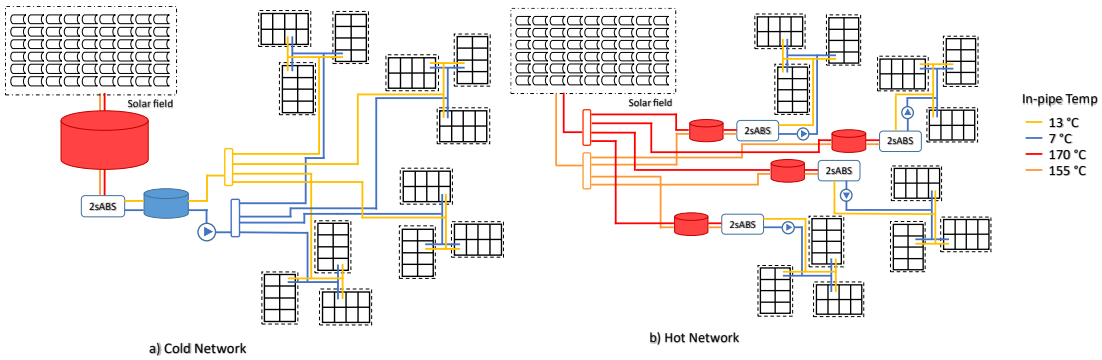

Figure 1. Schematization of the two configurations of Solar District Cooling: a) Cold network, b) Hot network.

conditions would dictate a higher flow rate than the maximum, a portion of the troughs must be sent to defocus.

$$\eta_{PTC} = A - B\frac{(\bar{T}-T_{amb})}{BTI \cdot CR} - C\frac{(\bar{T}-T_{amb})}{BTI \cdot CR} \quad (1)$$

$$BTI = DNI \cdot cos\theta \quad (2)$$

Hot water production is decoupled from use in the chiller by hot tanks. The fluid flow rate to the absorption machine is modulated to produce a temperature jump of 15°C. The supply water temperature has a tolerance between 155 and 170°C. A bypass controller, located between the storage tank and the chiller, adjusts the supply temperature to the chiller by mixing the supply and return flows from the chiller to maintain a temperature as close as possible to 170°C (design temperature). If the available temperature in the storage tank is below this set point, the bypass allows the supply to flow until the temperature falls below 155°C.

The performance of the absorption chiller (Li-Br 2sABS) is calculated for each operating condition according to the performance map provided by the manufacturer. The design point operating conditions are reported in Tab. 1and the effect of the chilled water set point is presented in Fig. 2. When the supply temperature from the chiller machine is above the setpoint of 7°C, an electric auxiliary cooling device is activated.

The heat from the condenser of the chiller is dissipated through an evaporative tower; in case the fluid leaving the CT has a temperature higher than 30°C, an exchange device with seawater intervenes to guarantee the set point condition. The type and number of components used in the two configurations are the same. The main difference is the temperature at which the fluid circulates in the distribution network. The network has identical flow and return lengths for a total of 20 km, while the diameter is calculated to limit the flow velocity inside the network to less than 3 m/s. In the case of the cold network, the circulating flow rate is a function of the load to be met by the utility, and an internal pipe diameter of 0.7 m with an insulation thickness of 86 mm is chosen. On the other hand, the hot network must be chosen based on the maximum flow rate that the solar system outlet can handle, while ensuring that the flow velocity does not exceed 3 m/s. The dimensions of the pipes and insulation should be selected based on (22) (23).

Table 1. Double stage Absorption Chiller performance (2.3 MW rated capacity)

	Parameters
Rated COP	1.39
Hot source range (°C)	2.0
Design chiller water (in-out) (°C)	7-14
Design hot water (in-out) (°C)	155-170
Design cooling water (in-out) (°C)	37-30

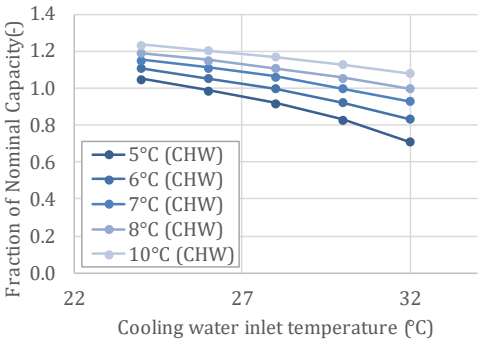

Figure 2. Effect of chilled water set point on rated performance

2.1 Location and cooling load demand

The system is assumed to be installed in Abu Dhabi, United Arab Emirates. The winter season in this area experiences mild temperatures due to the proximity of the sea. These areas have a warm climate, with temperatures consistently above 20 °C, except during the winter months, and reaching peaks around 45 °C in the summer. The humidity levels are quite high, which increases the heat load and hinders the performance of solar collectors by reducing direct radiation. The water exchanger operating conditions consider the seawater temperatures at various depths, using data provided by NOAA (National Oceanic and Atmospheric Administration).

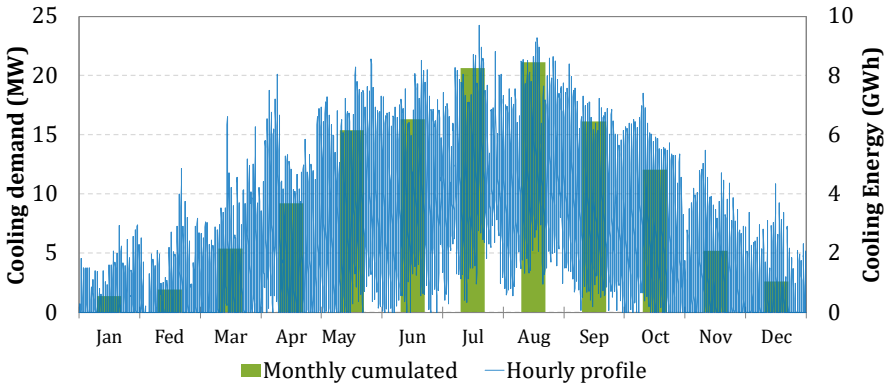

Figure 3. Cooling load of the entire agglomeration: annual hourly profile (blue) and monthly energy cumulated (green).

A detailed estimation of heat loads would require an evaluation of all components that contribute to the definition of sensible and latent loads, such as solar radiation, transmission through surfaces, infiltration of outside air, and the presence of people, lighting, and electrical equipment. However, since the focus of the following discussion is not specific to the building, a simplified load model is assumed that still accounts for typical daily and seasonal variations in cooling demand. As shown in Equation 1, the load is calculated as the sum of three components, a constant related to internal loads and two variables related to solar radiation and outdoor air temperature, respectively.

$$Q_{cool} = 2000 + \frac{5}{3} \cdot G + 850 \cdot (T_{amb} - 25) \quad (3)$$

With this definition, a peak load of 24 MW is obtained in July, which is comparable to a utility consisting of approximately 1300 houses of 100 m² each, assuming a maximum thermal load of 185 W/m² in this region (24). The annual trend of the demand is presented in Fig. 3.

2.2 Optimization

The objective is to determine the most cost-effective combination of power and component size for various solar fractions and both plant configurations. Solving such a complex problem typically necessitates a numerical approach due to the involvement of numerous independent variables. GenOpt software facilitates the minimization of an objective function, which is assessed by external software, specifically Trnsys in this case. A hybrid optimization algorithm is adopted, starting with a Particle Swarm Optimization on a largest mesh and refining the result with a Generalized Pattern Search, e.g., Hooke Jeeves algorithm.

The variables considered are: the capacity of the absorption chiller (P_{ABS}), the area of the solar array (S_{PTC}), and the volume of the high-temperature tank (V_{HWS}). The search space for optimization is outlined in Tab.2 with reference to the minimum and maximum values of each variable and the minimum considered variation in size. The objective function (Eq. 4) represents the investment cost of these three components, with an additional term to ensure the desired solar fraction is achieved ($Penalty_{SF}$). The unit cost of each component is listed in Tab. 2. It should be emphasized that the proposed economic evaluation does not provide a precise estimate of the installation costs, since it is intended only to compare the two scenarios, and therefore does not take into account all the common expenses, such as the piping grounding cost. The optimization procedure is repeated for four solar penetrations: 25%, 50%, 75 and 100%.

$$f_T(x) = C_{ABS} \cdot P_{ABS} + C_{PTC} \cdot S_{PTC} + C_{HWS} \cdot V_{HWS} + Penalty_{SF} \quad (4)$$

Table 2. Optimization search space and Specific cost of components

	Step value	Min value	Max value	Unit	Cost unit	
Absorption chiller	450	1800	19000	KW	560	$/kW
Solar collectors	2000	4000	60000	m²	480	$/m²
Hot water storage	100	20	1500	m³	2000	$/m³

3. Result and discussion

The outcomes of the optimization procedure for all considered configurations are displayed in Tab. 3 with respect to component size, and Fig. 4 offers a visual representation of the economic impact.

The results demonstrate a clear trend in both scenarios when considering SF≤75%. The cost of individual equipment, and consequently the cumulative cost, increases almost linearly with the solar fraction, although the values differ in the two cases. For the same amount of

annual cooling energy, the hot grid scenario requires a higher expense, primarily due to the necessity for a larger area of solar collectors. It is also noteworthy that this discrepancy remains relatively consistent, approximately 4-6 M$ on average. In the case of solar thermal energy alone (SF=100%), a significant change in trend is revealed. It can be seen that very high values of SF lead to a significant increase in cost, especially in solar array extension and storage tank size. This increase in cost is more pronounced in the cold-grid configuration, resulting in an overall cost that exceeds that of the hot-grid scenario. The additional expense is due to the larger storage volume, as the remaining parameters reach equivalent values.

Table 3. Technical optimization results: components size for the two configurations.

		SF 25	SF 50	SF 75	SF 100
Cold Network	Absorption chiller (kW)	3714	7739	13480	24607
	Solar collectors (m^2)	10971	23645	39022	106467
	Hot water storage (m^3)	250	614	969	10725
Hot Network	Absorption chiller (kW)	4122	8264	13607	24490
	Solar collectors (m^2)	19051	36084	48082	107300
	Hot water storage (m^3)	240	469	1009	8147

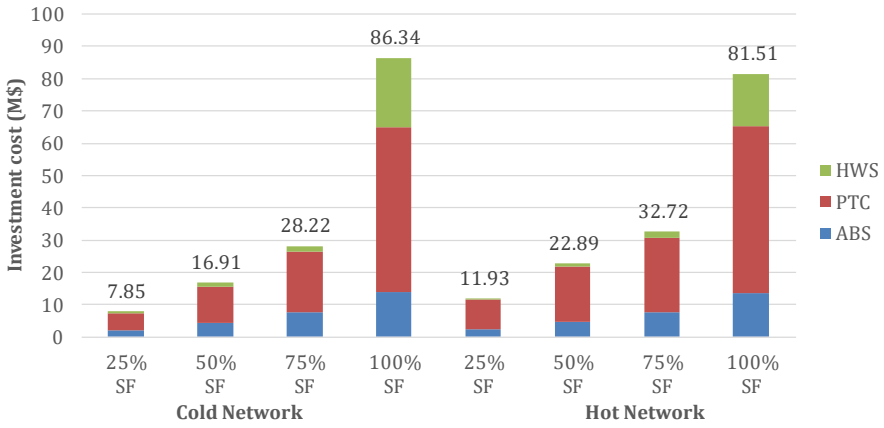

Figure 4. Economic optimization results: investment cost for the two configurations.

In order to gain a more comprehensive understanding of the outcomes of the optimization process, the average performance of the two most significant components, namely the solar array and the distribution network, is presented on an annual basis in Fig. 5. Starting from the cold-network scenario, an increase in SF necessitates a larger collector area, which in turn results in greater energy availability in terms of DNI intercepted by the solar field. However, the most significant consequences of choosing a larger solar fraction are reduced collector efficiency and increased heat loss at the storage. The former is essentially attributable to a higher temperature at the base of the storage, and thus of input to the PTCs, which in fact reduces the

hours of useful irradiance. Conversely, thermal losses at the storage are influenced not only by the average temperature of the fluid stored, but also by the overall surface area of the storage.

The trends of the chiller machine are not depicted in Fig. 5, but the recorded efficiency values are notably high. The average thermal efficiency, calculated as the ratio of cooling energy produced by the absorption technology alone to the input from the thermal source on an annual basis, reaches values just below 1.50, demonstrating remarkable stability even when the solar fraction varies.

With regard to the hot grid system, it is evident that there is a notable enhancement in heat dissipation at the distribution network, due to the substantial thermal gradient between the delivery fluid (180-200°C) and the ground. Consequently, up to 50% of the energy collected by the collectors is lost through the network. While this proportion decreases as the solar fraction increases, it never falls below 30%. The thermal efficiency of ABS remains essentially unchanged from the previous case. Consequently, in order to comply with the stipulated conditions for the SF, it is necessary to maintain a constant thermal input to the chiller. The collectors serve to compensate for the losses incurred through the grid, justifying a higher surface area of the solar array. However, losses in distribution result in a drop in the input temperature to the collectors, which, in light of the above, reflects positively on the efficiency of these components.

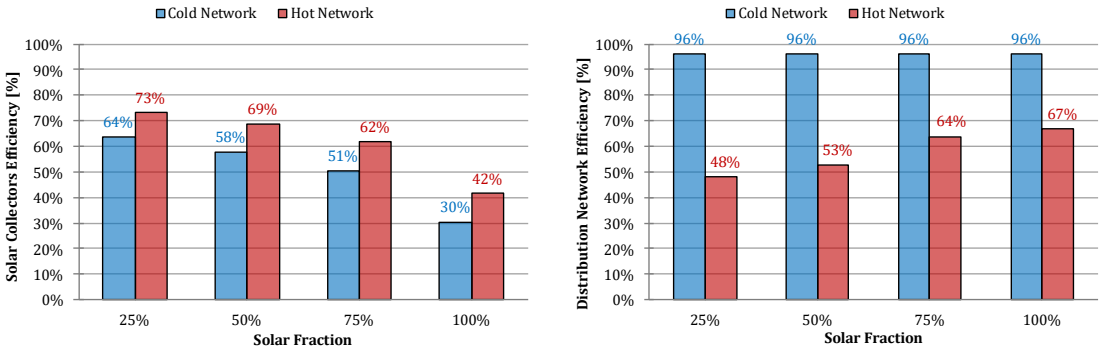

Figure 5. Economic optimization results: investment cost for the two configurations

4. Conclusion

The paper analyzed two configurations of district cooling with a chiller machine powered by a medium-high temperature solar collector with a hot water storage system. The two configurations differ in terms of the temperature of the transfer fluid. In the first configuration, the cold network, a chiller, which is in close proximity to the solar field, produces the chilled water for the entire network. In the second configuration, the hot network, the hot water at the exit of the solar array is sent through the network directly to smaller thermal storage tanks that serve local chillers and produce the chilled water for limited quarters. The size of the primary components of the system, including the chiller, thermal storage, and solar collector aperture, is optimized to minimize investment costs and achieve varying solar fractions.

Increasing the solar penetration of a system means increasing the chilled water production capacity of the system. This is generally reflected in components with a larger size. An increase in the solar fraction (SF) up to an SF of 75% is observed to result in a linear increase in the rate of change. However, higher SF reduces system performance due to the higher inlet temperature at the collectors. In fact, higher capturing power is reflected in higher average storage tank

temperature. In the event that the unit solar fraction (SF) is to be achieved, all components must be oversized in order to compensate for the variability in radiation availability. For instance, the solar array is more than twice the size of 75% SF, and the hot storage has 8/10 times the capacity. The distributed configuration does not appear to exert a particular influence on the size of the chiller. However, it does necessitate a larger opening of the mirrors, with an average of 50% for SFs smaller than 100%. The hot distribution network, which has a higher temperature, is characterized by larger heat losses. In order to guarantee the same heat input to the chiller, the solar array must be increased in proportion to the output. Conversely, in the full-solar scenario, the hot storage tank is 30% smaller in the distributed configuration. The distribution network upstream of the machine (not considered in the cost evaluation) provides an additional reserve of high-temperature fluid that allows the installation of a smaller volume of storage, resulting in significant savings.

The hot network is generally affected by higher losses, particularly through the distribution. However, the solar field shows better performance, which shifts the point of convenience for the fully solar scenario.

Nomenclature

ABS	Absorption Chiller	DC	District Cooling	SDC	Solar-assisted District Cooling
BTI	Beam Total Irradiance	DNI	Direct Normal Irradiance	SF	Solar Fraction
CHW	Chilled Water	G	Total Solar Radiation	T	Temperature
COP	Coefficient Of Performance	HWS	Hot Water Storage	η_{PTC}	Concentrator thermal efficiency
CR	Concentration Ratio	PTC	Parabolic Trough Collector	θ	Concentrator Incidence Angle
CT	Cooling Tower	Q_{cool}	Cooling Demand	2sABS	Double Stage Absoprtion Chiller

References

1. Alotaibi S, Alhuyi Nazari M. District cooling in the Middle East & North Africa; history, current status, and future opportunities. J Build Eng. ottobre 2023;77:107522.

2. Inayat A, Raza M. District cooling system via renewable energy sources: A review. Renew Sustain Energy Rev. giugno 2019;107(March 2019):360–73.

3. Brumana G, Franchini G, Ghirardi E. Potential of solar-driven cooling systems in UAE region. Sol Energy Adv. 2022;2:100025.

4. Alghool DM, Elmekkawy TY, Haouari M, Elomri A. Optimization of design and operation of solar assisted district cooling systems. Energy Convers Manag X. aprile 2020;6(August 2019):100028.

5. Eveloy V, Ayou DS. Sustainable district cooling systems: Status, challenges, and future opportunities, with emphasis on cooling-dominated regions. Energies. 2019;12(2).

6. Brumana G, Franchini G, Ghirardi E. Optimization and performance assessment of a solar district cooling system. In: AIP Conference Proceedings [Internet]. 2019. p. 020026. Disponibile su: http://aip.scitation.org/doi/abs/10.1063/1.5138759

7. Broadstock DC, Wang X. District cooling services: A bibliometric review and topic classification of existing research. Renew Sustain Energy Rev. febbraio 2024;190:113893.

8. Østergaard PA, Werner S, Dyrelund A, Lund H, Arabkoohsar A, Sorknæs P, et al. The four generations of district cooling - A categorization of the development in district cooling from origin to future prospect. Energy. agosto 2022;253:124098.

9. Michaelides EE. Thermal Storage for District Cooling—Implications for Renewable Energy Transition. Energies. 4 novembre 2021;14(21):7317.

10. Al-Nini A, Ya HH, Al-Mahbashi N, Hussin H. A Review on Green Cooling: Exploring the Benefits of Sustainable Energy-Powered District Cooling with Thermal Energy Storage. Sustainability. 20 marzo 2023;15(6):5433.

11. Thakar K, Patel R, Patel G. Techno-economic analysis of district cooling system: A case study. J Clean Prod. settembre 2021;313:127812.

12. Shi X, Qian Y, Yang S. Fluctuation Analysis of a Complementary Wind–Solar Energy System and Integration for Large Scale Hydrogen Production. ACS Sustain Chem Eng. 11 maggio 2020;8(18):7097–110.

13. Dai W, Xia W, Li B, Goh H, Zhang Z, Wen F, et al. Increase the integration of renewable energy using flexibility of source-network-load-storage in district cooling system. J Clean Prod. gennaio 2024;140682.

14. Lepiksaar K, Mašatin V, Krupenski I, Volkova A. Effects of Coupling Combined Heat and Power Production with District Cooling. Energies. 6 giugno 2023;16(12):4552.

15. Neri M, Guelpa E, Verda V. Design and connection optimization of a district cooling network: Mixed integer programming and heuristic approach. Appl Energy. gennaio 2022;306:117994.

16. Zhang W, Jin X, Zhang L, Hong W. Performance of the variable-temperature multi-cold source district cooling system: A case study. Appl Therm Eng. agosto 2022;213:118722.

17. Jangsten M, Filipsson P, Lindholm T, Dalenbäck JO. High Temperature District Cooling: Challenges and Possibilities Based on an Existing District Cooling System and its Connected Buildings. Energy. maggio 2020;199:117407.

18. Guelpa E, Bellando L, Giordano A, Verda V. Optimal Configuration of Power-to-Cool Technology in District Cooling Systems. Proc IEEE. settembre 2020;108(9):1612–22.

19. Cozzini M, D'Antoni M, Buffa S. District Heating and Cooling Networks Based on Decentralized Heat Pumps: Energy Efficiency and Reversibility at Affordable Costs. 2018;

20. Brumana G, Franchini G, Ghirardi E. Performance Assessment of Solar Cooling Systems with Energy Storage. ATI Italian Termotecnics Association, ATI Italian Termotecnics Association, curatori. E3S Web Conf. 2021;312:08014.

21. Brumana G, Franchini G, Ghirardi E, Perdichizzi A. Analysis of Solar District Cooling systems: the Effect of Heat Rejection. E3S Web Conf. ottobre 2020;197:08018.

22. Lund R, Mohammadi S. Choice of insulation standard for pipe networks in 4th generation district heating systems. Appl Therm Eng. 2016;98:256–64.

23. Kristjansson H, Bøhm B. Advanced and traditional Pipe systems: Optimum Design of Distribution and service Pipes. 10th Int Symp Dist Heat Cool. 2006;11.

24. Brumana G, Franchini G. Solar-Powered Air Conditioning for Buildings in Hot Climates: Desiccant Evaporative Cooling vs. Absorption Chiller-based Systems. Energy Procedia. 2016;101(September):288–96.